

Three-dimensional finite element analysis of bio-inspired root anchored pile in clay

Yonathan Prasetya Ongkowijoyo¹, Aswin Lim^{1*}, and Ryan Alexander Lyman¹

¹Department of Civil Engineering, Universitas Katolik Parahyangan, Bandung, 40141, Indonesia

Abstract. This paper examines the pile bearing capacity of the innovative pile foundation, which is inspired by razor clam and the anchorage of tree root, so-called Bio-inspired Root Anchored Pile (BRAP). Three-dimensional finite element analysis was conducted by making use of a well-documented pile load test in North Jakarta. The results showed that, the BRAP pile could increase the pile bearing capacity from 14.7% to 25% if compared with the conventional pile foundations. In addition, the contribution of the BRAP anchor bolt is around 6 to 9% of the total load. This indicates that the BRAP could be an alternative solution to overcome the soft soil problem instead of increasing the conventional pile dimension, such as length and diameter.

1 Introduction

In the last decade, geotechnical engineering has begun to take inspiration from biology and has given a new branch of science called biogeotechnics. Biogeotechnics is an interdisciplinary of geotechnical engineering and biology that focuses on developing bioinspiration and biomediation-based technologies to be applied to engineering. Several biogeotechnical discoveries include the use of biopolymers for soil bioremediation [1], Fungi-treated soil [2-4], self-driving robots inspired by bamboo shells [5], as well as innovations in the form and mechanism of pile foundations [6].

Extending the pile penetration till it reaches the hard soil layer is a common practice for enhancing the bearing capacity of the pile foundation. Nevertheless, the use of such a typical technique is thought to be less successful in soil conditions with relatively deep hard soil depths, and it tends to raise the costs of pile foundation building.

To address the limitations of the typical technique described above, Aleali et al. [6] proposed three unique concepts to increase the friction resistance capability of pile foundations inspired by living organisms, including bamboo shells, earthworms, and tree roots or seaweed. Bioinspired Radially Expansive Pile (BREP), Bioinspired Setae Anchored Pile (BSAP), and Bioinspired Root Anchored Pile (BRAP) are the three concepts [6]. One of the above-mentioned developments, the Bioinspired Root Anchored Pile (BRAP), will be numerically modeled in this article utilizing software based on the PLAXIS 3D finite element method.

2 Background theory

Biomediation is the application of biological processes and/or systems that create bio-geochemical processes to modify the physical and mechanical characteristics of soil in the context of geotechnical engineering. [7]. For example, Lim et al 2021 [1] used fungi to enhance the shear strength of loose sand soils, Martinez et al 2013 [8] used microbiologically induced calcium carbonate precipitation (MICP), Chou et al 2011 [9] used ureolysis to bio-calcify sand, and so on.

Meanwhile, bio-inspiration or bio-mimicry is the technique of incorporating ideas from nature into technological innovation [10]. The method of adopting bioinspiration consists of two main phases: examining living things, particularly in terms of shape, behavior, and principles, and selecting challenges to be solved [11]. The order of these two steps divides the bioinspiration process into two systematic approaches: solution-based and problem-based [6]. The shape level discusses an organism's physical and structural components, the behavioral level examines an organism's function and interaction including its environment, and the principal level explores the reasons, purposes, or uses of an organism's appearance and behavior in its environment. Fig. 1 depicts a bioinspiration example for each of the three levels. The bioinspiration process adopts the architectural shape of tree roots at the form level, while the behavior level adopts the pattern or technique of development and branching of tree roots, and the principal level follows plant principles in terms of storing resources and employing them when needed [12].

Form adoption is at the lowest level of abstraction, followed by behavior and principles. The lower the degree of abstraction of bioinspiration that may be necessary, the

*Corresponding author: aswinlim@unpar.ac.id

more comparable the conditions that arise between the engineering challenges faced and the biological processes under consideration. The greater the disparity between the technical issues encountered and the biological

phenomenon under investigation, the more in-depth the study required to extract biological methods [10].

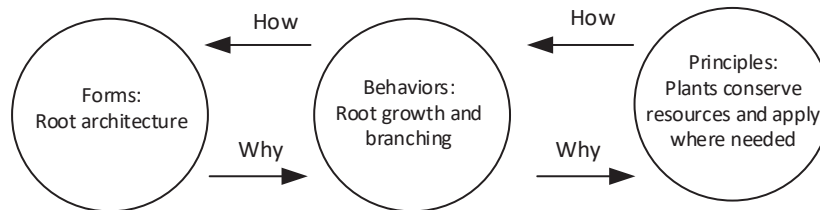


Fig. 1. The adoption level of the bio-inspiration process diagram [12].

Bioinspired Root Anchored Pile (BRAP) is an innovation that modifies drilled piles designed as friction resistant piles. Inspired by the split exoskeleton of bamboo shells and anchorage from tree roots, BRAP is made by using split tubes inserted into drilled holes which are then bolted to the sides of the ground along the poles, then filled with reinforced concrete. The aim of this innovation is to increase the friction capacity of the pile. The schematic diagram of BRAP is illustrated in Fig. 2. Fig 2 (a) and 2 (b) are adopted from Aleali et al. [6].

but can be rotated up to a certain degree. Any external force acting on the tree will cause the roots to rotate slightly. The slightest movement of these roots will cause the surrounding soil to compact as well. Trial to apply this mechanism in BRAP anchorage by making the connection between the split tube plate and the anchor bolt have a certain degree of flexibility so that when the pile is subjected to axial load the anchor bolt can rotate slightly and compact the soil around it a little [13].

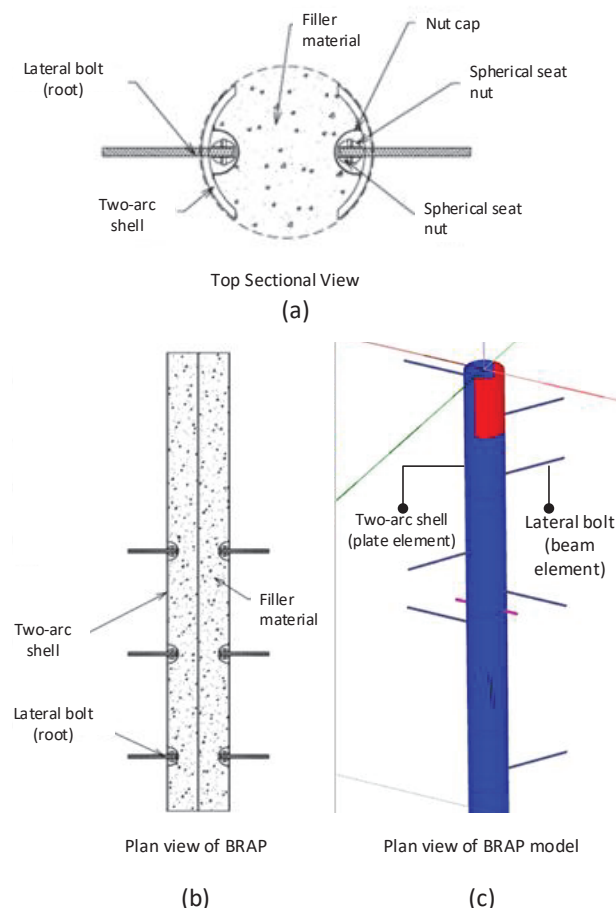


Fig. 2. Schematic diagram of BRAP (a) top sectional view, (b) plan view, and (c) model plan view.

BRAP anchorage is designed based on inspiration from tree roots in the ground that spread in a horizontal direction. In the process of growth, tree roots will try to penetrate the softer layer of soil. Then, when the roots have entered the soil layer and then the roots grow bigger, the surrounding soil will compact because of it. In addition, the root connection with the tree body is not rigid

3 Modelling procedure

A well-documented pile load test located in North Jakarta was simulated to numerically the effectiveness of the BRAP [14]. The soil layers consist of six layers and the three-dimensional mesh for analysis is shown in Fig. 3.

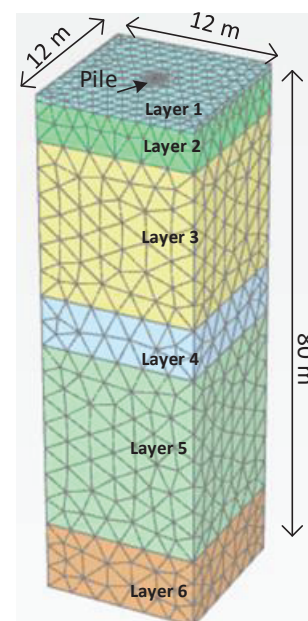


Fig. 3. Three-dimensional mesh for analysis.

A 1-m thick first layer is very soft silty clay with $N_{average}$ is 2. Then, a loose sand layer is founded between -1 m to -7 m with $N_{average}$ is 8. The third layer is the predominant layer, which is consist of very soft clay until -31 m with $N_{average}$ is 2. Afterward, the fourth, fifth, and sixth layers are dense sand, hard silty clay, and medium sand, respectively. In total, the depth of simulated soil layers is 80 m. The vertical boundaries were constrained in the horizontal direction, and the bottom boundary was constrained in all directions. The x and y axis is 12 m, and

it is considered enough to minimize the boundary effect because the distance is about 20 times of pile diameter. The pile is modeled wish-in-place. The simulation stages of BRAP is listed in Table 1.

Table 1. The simulation stages of BRAP.

Stage	Activities
0	Initial condition
1	Activate pile
2	Reset displacement to zero
3	Activate Load until failure

3.1 Soil constitutive model

The Hardening Soil (HS) model [15] is a true second-order model for soil in general (soft to stiff types of soil). The model uses cap hardening characteristics to simulate the plastic volumetric strain in primary compression and frictional hardening characteristics to simulate the plastic

shear strain in deviatoric loading. A failure is defined by the Mohr-Coulomb failure criterion. The major features of the model are a Mohr-Coulomb failure with input parameters c , f and dilatancy angle, ψ , stress-dependent stiffness according to a power law defined by input parameter, m , plastic straining resulting from primary deviatoric loading with an input parameter, E_{50}^{ref} , and plastic straining from primary compression with an input parameter E_{oed}^{ref} , elastic unloading/reloading is defined by input parameters E_{ur}^{ref} and unloading/reloading Poisson's ratio, ν_{ur} .

Fig. 4 displays the shear yield surface and cap yield surface in the Hardening Soil Model for soil with no cohesion ($c'=0$). The soil yield is defined as the stress state of soil which is located in the shear hardening zone. Meanwhile, the soil failure is defined as the stress state of soil which reaches to the Mohr-Coulomb failure line.

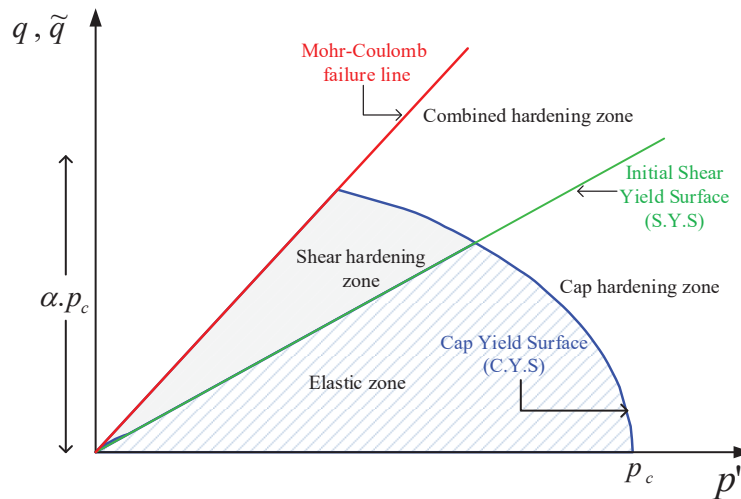


Fig. 4. The shear yield surface and cap yield surface in the hardening soil model for soil [15].

Furthermore, Fig. 5 illustrate the hyperbolic stress-strain relation in primary loading for a standard drained triaxial test and oedometer test, respectively, to express the definition of E_{50}^{ref} , E_{ur}^{ref} , and E_{oed}^{ref} . The input parameters of soil are listed in Table 2.

3.2 Structural Element Model

The two-arc shell of BRAP was modeled using a plate element. Meanwhile, the lateral bolt was modeled using two types of elements, namely beam and embedded beam elements. The objective is to investigate which element is appropriate to model the lateral bolt (Fig. 2c). The structural elements were modeled as linear elastic material with the main inputs are Young's modulus (E_c) and Poisson ratio (ν). The input parameters of structural elements are listed in Tables 3-4.

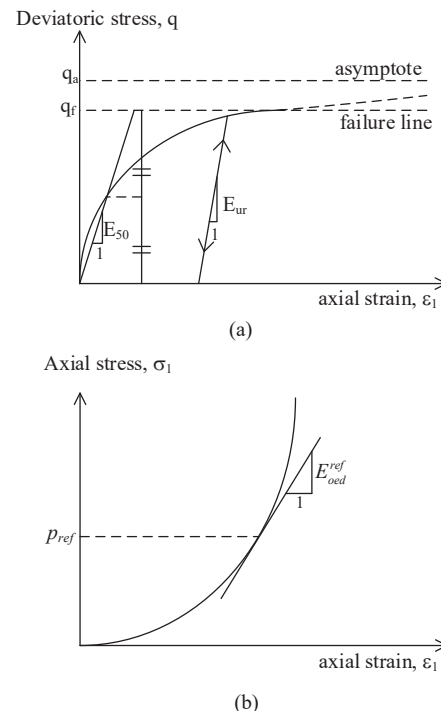


Fig. 5. The hyperbolic stress-strain relation in primary loading for a standard drained triaxial test and oedometer test [15].

Table 2. Input parameters for soil.

Soil Strata	Depth (m)	$N_{average}$	γ (kN/m ³)	c [kN/m ²]	ϕ [°]	E_{50}^{ref} [kN/m ²]	E_{oed}^{ref} [kN/m ²]	E_{ur}^{ref} [kN/m ²]	m	ν_{ur}
Very soft - silty clay	0-1	2	17	0	25	1000	1000	3000	1	0.35
loose - sand	1-7	8	18	0	27	3000	3000	9000	1	0.35
Very soft - silty clay	7-31	2	17	0	25	1000	1000	3000	1	0.35
Dense - sand	31-39	32	21	0	34	32000	32000	96000	0.5	0.3
Hard - silty clay	39-69	26	20	0	31	20000	20000	60000	0.5	0.3
Medium - sand	69-80	27	21	0	30	28000	28000	84000	0.75	0.3

Table 3. Input parameters for the plate element.

Material Type	Elastic
Material	Steel
Length	44.5 m
Diameter	0.6 m
Thickness	0.1 m
Unit weight	77 kN/m ³
Young's modulus	200 GPa

Table 4. Input parameters for the beam element.

Material Type	Elastic
Material	Baja
Length	0.2 m
Diameter	0.02 m
Unit weight	78.5 kN/m ³
Young's modulus	200 GPa
Vertical spacing	4 m
Axial skin resistance (embedded beam)	Layer dependent

4 Result and discussion

Fig. 6 shows the comparison of the measured and computed load-settlement curve for the conventional bored pile. It is clearly seen that the computed result is very close to the measured data. It indicates that the input parameters for soil and structural elements have been successfully verified. Moreover, the 3D model also validated properly.

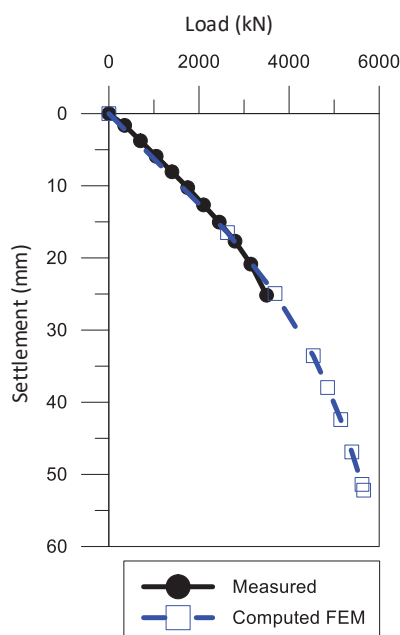


Fig. 6. The comparison of measured and computed load-settlement curve.

Next, the BRAP was simulated numerically by simply changing the pile conventional pile model to the BRAP pile model. Here, the anchor bolt was modeled with two types of elements, such as the beam and the embedded beam element. Fig. 7 shows the comparison of the conventional bored pile and the BRAP load-settlement curves. It is clearly seen that the load-settlement curve of the BRAP pile moved to the right-side. It indicates that the pile capacity increased. The ultimate load of the conventional bored pile is 5994 kN, meanwhile, the BRAP failure load in which modeled with Beam and Embedded Beam is 6873 kN and 6876 kN. It could be said that the pile capacity increased about 14.7%. Moreover, the anchor bolt could be modeled either beam or embedded beam elements. Those two elements did not yield a major difference.

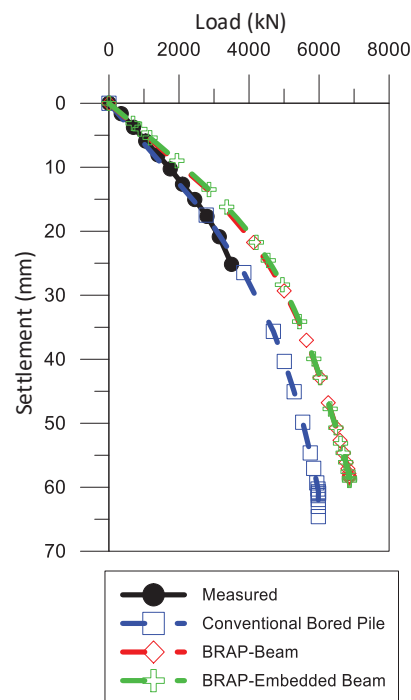


Fig. 7. The comparison of conventional bored-pile and brap load-settlement curves.

Furthermore, the load distribution acting on the BRAP pile could be examined. The load was bear by the pile tip (Q_p), the pile sleeve (Q_s), and the anchor bolt (Q_{ab}). Each load proportions are listed in Table 5. It could conclude that the anchor bolt is contribute around 6-9 % of the total load acting on the pile. This value might be higher if the length of anchor bolt longer, or the spacing of anchor bolt could be closer. Those components are undergoing study and the results might be presented in the next publication.

Table 5. The load distribution of BRAP

Pile Type	Ultimate load (kN)	Load Distribution		
		Qs [kN]	(Qp + Qab) [kN]	Qab [kN]
Conventional Pile	5994	5056	938	0
BRAP - <i>Beam</i>	6873	5285	1588	650
BRAP - <i>Embedded Beam</i>	6876	5344	1532	594

5 Conclusions

Based on the three-dimensional finite element analyses results, the pile capacity of the conventional pile and BRAP are investigated. The results shows that the BRAP could increase the pile capacity about 14.7% with 6-9% load distribution was come from the anchor bolt. In the future, the dimension of the anchor bolt and the spacing of the anchor bolt are worth to be studied. In addition, BRAP also worth to be tested in the full-scale, and the construction of BRAP pile also worth to be examined.

The author acknowledges the support provided by Parahyangan Catholic University and PT Pakubumi Semesta for the provision of geotechnical information in the case study.

References

1. A. Lim, M.R. Iskandar, Y. Albrecht, IOP Conf. Ser.: Earth Environ. Sci. **871**, 012056 (2021) DOI 10.1088/1755-1315/871/1/012056
2. A. Lim, P.C. Atmaja, S. Rustiani, Journal of Rock Mechanics and Geotechnical Engineering **12**(1), 180-187 (2020) <https://doi.org/10.1016/j.jrmge.2019.09.004>
3. A. Lim, L. Pianica, Jurnal Aplikasi Teknik Sipil **20**(2), 157-162 (2022) <http://dx.doi.org/10.12962/j2579-891X.v20i2.9769>
4. A. Lim, P. Henzi, O. Arvin. Journal of GeoEngineering **18**(1), 1-10 (2023)
5. J. Tao, S.C. Huang, Y. Tang, Journal of Geotechnical and Geoenvironmental Engineering **145**(12), 02819002 (2019) [https://doi.org/10.1061/\(ASCE\)GT.1943-5606.0002177](https://doi.org/10.1061/(ASCE)GT.1943-5606.0002177)
6. S. Aleali, P. Bandini, C. Newton. J Bionic Eng **17**, 1059-1074 (2020) <https://doi.org/10.1007/s42235-020-0076-6>
7. J.T. DeJong, E. Kavazanjian, Geotechnical Fundamentals for Addressing New World Challenges, 193-207 (2019) https://doi.org/10.1007/978-3-030-06249-1_7
8. B.C. Martinez, J.T. DeJong, T.R. Ginn, B.M. Montoya, T.H. Barkouki, C. Hunt, B. Tanyu, D. Major, Journal of Geotechnical and Geoenvironmental Engineering **139**(4), 587-598 (2013) [https://doi.org/10.1061/\(ASCE\)GT.1943-5606.0000787](https://doi.org/10.1061/(ASCE)GT.1943-5606.0000787)
9. C.W. Chou, E.A. Seagren, A.H. Aydilek, M. Lai, J Geotech Geoenviron **137**(12), 1179-1189 (2011)
10. J. Vincent, International Centre for Mechanical Sciences **412**, 51-58 (2001) https://doi.org/10.1007/978-3-7091-2584-7_3
11. T.W. Mak, L.H. Shu, CIRP Annals **53**(1), 117-120 (2004) [https://doi.org/10.1016/S0007-8506\(07\)60658-1](https://doi.org/10.1016/S0007-8506(07)60658-1)
12. J.T. DeJong, M. Burrall, D.W. Wilson, J.D. Frost. Geotechnical Frontiers (2017) <https://doi.org/10.1061/9780784480472.092>
13. A. Martinez, J.T. DeJong, I. Akin, A. Aleali, C. Arson, J. Atkinson, P. Bandini, T. Baser, R. Borela, R. Boulanger, M. Burrall, Y. Chen, C. Collins, D. Cortes, S. Dai, E.D. Dottore, K. Dorgani, R. Fragaszy, J.D. Frost, R. Full, M. Ghayoomi, D.I. Goldman, N. Gravish, I.L. Guzman, J. Hambleton, E. Hawkes, M. Helms, D. Hu, L. Huang, C. Hunt, D. Irschick, H.T. Lin, B. Lingwall, A. Marr, B. Mazzolai, B. McInroe, T. Murthy, K. O'Hara, M. Porter, S. Sadek, M. Sanchez, C. Santamarina, L.S. Shao, J. Sharp, H. Stuart, H.H. Stutz, A. Summers, J. Tao, M. Tolley, L. Treers, K. Turnbull, R. Valdes, L.V. Paassen, G. Viggiani, D. Wilson, W. Wu, X. Yu, J.X. Zheng, Géotechnique **72**(8), 687-705 (2021) <https://doi.org/10.1680/jgeot.20.P.170>
14. A. Lim, V.H. Batistuta, Y.V. Wijaya. Journal of the Civil Engineering Forum **8**(1), 21-30 (2022) <https://doi.org/10.22146/jcef.3597>
15. T. Schanz, P.A. Vermeer, P.G. Bonnier, *The hardening soil model: formulation and verification*, in Beyond 2000 in Computational Geotechnics, 281-290 (Routledge, 1999)